

# Spatio-Temporal Changes in the World Largest Mangrove Forest and Human Perceptions in Bangladesh: A Study Using GIS-RS and Social Survey Techniques

Muhammad Esmat Enan<sup>1</sup>, Naznin Bintey Hayder<sup>2</sup>, Sazzadul Eanan<sup>3</sup>, Md. Faruk Hossain<sup>4\*</sup> and Md. Ahasanul Hoque<sup>5</sup>

<sup>1</sup> Institute of New Imaging Technologies, Universitat Jaume I, Castellón de la Plana, Castellón 12071, Spain

<sup>2</sup> Department of Innovation of Biological Systems, Food and Forestry (DIBAF), Tuscia University, Viterbo, Italy

<sup>3</sup> Department of Geography and Environmental Studies, University of Chittagong, Bangladesh

<sup>4</sup> Department of Geography and Environment, University of Dhaka, Dhaka 1000, Bangladesh

<sup>5</sup> Geospatial and Data Management Specialist, UNDP, Bangladesh

*Manuscript received: 20 June 2023; accepted for publication: 12 October 2023*

**ABSTRACT:** Mangrove forests are disappearing at a faster rate than any other forests in many places around the world due to natural and anthropogenic causes; as a result, natural resources are decreasing. Considering these issues, present study focuses on the changing pattern of the world's largest mangrove forest which locally known as Sundarbans, and utilized Landsat satellite imagery during the periods 2000 to 2021 as the primary data source. Using Google Earth Engine, the Normalized Difference Vegetation Index (NDVI) was applied to classify the images into 4 LULC categories (water bodies, sediment, forest, and others). The accuracies of the image classifications were between 89.76 and 92.21 percent. Classified images for the years 2000, 2010, and 2021 were then used to train and validate the ANN-CA (artificial neural network-based cellular automaton) model applied to produce the LULC scenario for the year 2031. On the other hand, a questionnaire survey was conducted in Sarankhola, and Shyamnagar Upazila to identify locals' perceptions of the causes of LULC changes in the study area. The findings reveal a great change from 4036.92 to 3969.33 km<sup>2</sup> of forest cover between 2000 and 2021, and further degradation of 3913.03 km<sup>2</sup> by the projected year (2031). The results show that all the 13 identified causes are driving the LULC changes in Sundarbans. The study also suggests if the appropriate management practices are not implemented, the study area's forest land degradation will likely continue in the years to come.

**Keywords:** Sundarbans; ANN-CA; NDVI; GEE; Mangrove Forest; LULC

## INTRODUCTION

The mangrove forest encompasses 15,000,000 ha, making it one of the world's most pristine ecosystems (Spalding et al., 2010; Biswas and Biswas, 2019; Carugati et al., 2018). Mangroves offer crucial environmental and societal commodities and services (Giri et al., 2007). This intertidal forest is one of the most effective terrestrial carbon sinks, capable of sequestering two to four times more carbon than mature tropical forests (Rahman et al., 2015). Despite their significance, mangrove forests are decreasing at 1–2% rate each year across the world (Spalding et al., 2010). In the last 20 years, the rate of loss has climbed to 35%

(Carugati et al., 2018; FAO, 2007; Polidoro et al., 2010; Giri et al., 2010).

Due to its critical significance, every mangrove forest is essential, and the Sundarbans is no exception (Chowdhury and Hafsa, 2022). The Sundarbans is the biggest mangrove forest on earth, is located in a region that is shared by Bangladesh and India (Ghosh et al., 2015). The Sundarbans currently covers an area of 10,000 km<sup>2</sup>, 60% of it is in Bangladesh and the rest in India, and in Bangladesh portion, millions of citizens receive benefit from coastal protection provided by the Sundarbans (Giri et al., 2007). The Sundarbans in Bangladesh are affected by serious cyclones, massive quantities of sediments taken by the river, and salinity concentrations change over a wide range of spatio-temporal scales (Gopal and Chauhan, 2006). Therefore, the fundamental natural and anthropogenic factors that affect the patterns of land use land cover change must be carefully interpreted to understand the spatio-temporal evolution

---

\* Corresponding Author: Md. Faruk Hossain

Email: faruk.geoenv@du.ac.bd

DOI: <https://doi.org/10.3329/dujecs.v12i1.70558>

of LULC patterns in the coastal regions of Bangladesh, especially the Sundarbans (Sarwar and Woodrofe, 2013; Abdullah et al., 2019).

Globally, numerous attempts have been made to detect mangrove forest change using Landsat time series data (Hasan et al., 2020). However, for effective management of mangrove wetland resources with satellite images and remote sensing methods, a comprehensive LULC change analysis is required (Orimoloye et al., 2020; Zaldo-Aubanell et al., 2021; Faruque et al., 2022) and in the past few years, many studies in Bangladesh have been conducted on mapping and LULC change estimation by applying GIS techniques (Mehta et al., 2012; Rawat and Kumar, 2015; Faruque et al., 2022). Several studies have also been undertaken to focus on land cover transformation in the Sundarbans, but earlier studies produced contradictory findings, underscoring the demand for more investigation (Quader et al., 2017). Besides, insufficient research has been done in the selected study area to identify the factors contributing to LULC dynamics (Akbar Hossain et al., 2022; Islam et al., 2019) especially, involving the local people, who can trace the root causes of these dynamics. As a result, monitoring, analysis, and simulating the scenario of land use and land cover (LULC) are crucial for activities related to conservation, planning, ecosystem management, and decision-making (Hasan et al., 2020; Parsa et al., 2016; Halmy et al., 2015).

Among the different approaches established to date for forecasting and modeling LULC changes, models based on statistical techniques like Markov chain, and cellular approaches are the most popular (Baig et al., 2022; Zeshan et al., 2021; Mountrakis, 2011; Shamsi, 2010). The Artificial-neural-network-based cellular automaton (ANN-CA) is a nonlinear technique that uses a bottom-up approach and many output neurons to simulate various changes in land use (Debanshi and Pal, 2020; Li and Yeh, 2002). It is well acknowledged that ANN can produce outcomes with more accuracy in modeling since they are highly capable of dealing with flawed and imperfect data and capturing non-linear, complicated aspects in modeling processes (Yang et al., 2015; Li and Yeh, 2002). ANN-CA was, therefore, determined to be the optimum option for simulating the Sundarbans' potential future in this study. Taking everything into account, the study aims to apply geospatial and questionnaire survey techniques to estimate the LULC changes in Sundarbans and identify the root causes of that LULC changes. The study's particular goals therefore, are i)

Investigation of spatiotemporal transformation in LULC of the Sundarbans and ii) Identification of root causes of LULC changes based on local people's perception.

## MATERIALS AND METHODS

### Study Area

The Sundarbans (Fig. 1) represent the largest continuous block of mangroves in the world, stretching 6,017 km<sup>2</sup> along Bangladesh's coast and 4,000 km<sup>2</sup> along India's (Sarker et al., 2016). The four administrative divisions that makeup Bangladesh's entire Sundarbans region are the Sarankhula, Chandpai, Khulna, and Sathkhira ranges (Quader et al., 2017).

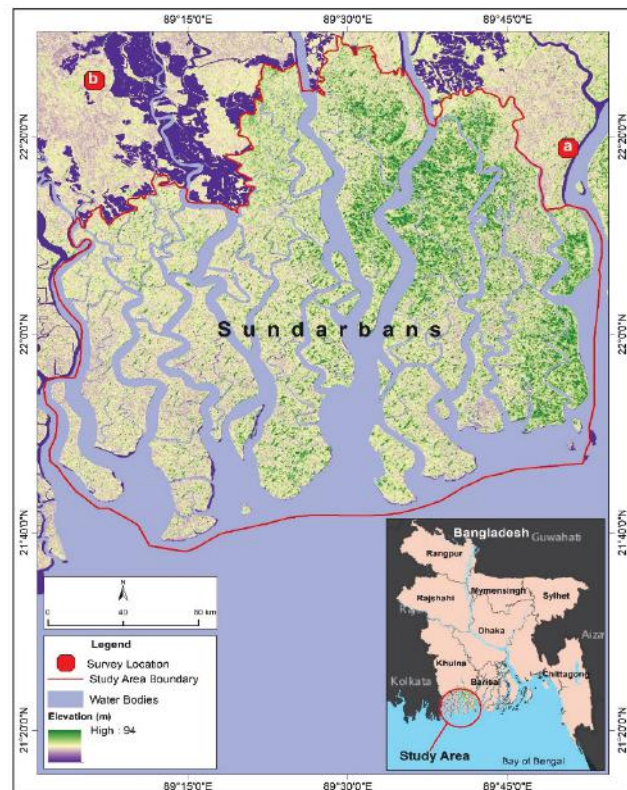


**Figure 1:** Study Area: Total Area within the Selected Boundary is about 5902.42 sq km (Two Red Points (“a” and “b”) on the Map Represent the Location of Sharankhola Upazila (Lat: 22.3129, Long: 89.8480) and Shyamnagar Upazila (Lat: 22.337299, Long: 89.108650). The Questionnaire Survey was Conducted in These Two Upazila)

**Data Collection**

Google Earth Engine (GEE) has proven to be useful over conventional software interfaces in processing bulky earth observatory data. Based on the GEE, for the current study, calibrated top-of-atmosphere (TOA) reflectance Landsat 5 and Landsat 8 images collected from January to March for the years 2000, 2007, 2010, 2016, and 2021 were collected. As these datasets consider the atmospheric variables and changes in the sun’s angle, these improve measurement accuracy and consistency across time and scenes. On the other hand, the simulation model used in this study requires some auxiliary data to predict the future scenario; therefore, five auxiliary data were utilized. Among these five auxiliary data, elevation, slope, and aspect data were prepared from Shuttle Radar Topography Mission (SRTM) version 3, which was collected from EarthExplorer (usgs.gov), and the two other auxiliary data were the distance from sea and distance from river. These auxiliary data help to enhance a model performance. Apart from these, a questionnaire survey was carried out in Sarankhola (Bagerhat), and Shyamnagar (Satkhira) upazila to identify the driving factors of changes in LULC of the Sundarbans among the 80 respondents.

**Data Processing**

For satellite-based change detection, NDVI (Normalized Difference Vegetation Index) was calculated for the selected years based on the following formula (USGS, 2022).

$$NDVI = \frac{(NIR - Red)}{(NIR + Red)} \dots\dots\dots i$$

This is a common formula to illustrate the NDVI concept, but band characteristics vary according to the satellite capturing earth observatory information. So, the adopted NDVI equations for Landsat 5 and Landsat 8 can be expressed as follow (USGS, 2022).

$$NDVI_{L5} = (Band\ 4 - Band3)/(Band\ 4 + Band3) \dots\dots ii$$





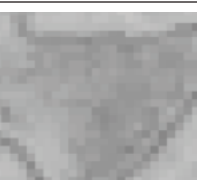



Where  $NDVI_{L5}$ = Normalized Difference Vegetation Index from Landsat 5.

$$NDVI_{L8} = (Band\ 5 - Band4)/(Band5 + Band4) \dots\dots\dots iii$$

Where  $NDVI_{L8}$ = Normalized Difference Vegetation Index from Landsat 8.

All the NDVI outputs were exported to Google Drive from GEE. These exported images then were classified depending on NDVI value in ArcGIS 10.8 (Table 1). Using Google Earth Pro, post-classification accuracy analyses were performed on all of the classified images. Calculations were made for the overall accuracy, user accuracy, producer accuracy, and Kappa coefficient. Overall accuracy is defined as the percentage of correctly classified pixels in an image out of all pixels. On the other hand, the kappa coefficient ranges from -1 to 1. A value around 1 suggests that the classification is substantially more accurate.

**Table 1:** Specification of the Land Use Classification Schema (All Images were Classified into Four Classes; Each Class is Representing a Different Land Cover. The Table is Prepared Depending on the NDVI Values for the Year 2000)

Classes	NDVI Value		NDVI Map View	True Colour Map View	Specification
	From	To			
Water	-0.889	-0.072			Sea, river, canal
Sediment	-0.071	0.169			Deposited sediment, mud or soil
Others	0.170	0.366			Bare land and constructed land
Forest	0.367	0.972			Mangrove forest

In the next step, the auxiliary data (elevation, slope, aspect, and distance from the sea and distance from the river) were prepared using ArcGIS 10.8. While preparing these data, the spatial reference system and data extent of NDVI outputs were followed, as the selected prediction model requires geometrics similarity among the inputs (variables).

**Simulation of LULC in Sundarbans**

An ANN-CA model with three layers— output layer, hidden layer, and input layer—was used to simulate the LULC. The selection of the inputs marked the beginning of the process. In this case, the land use scenarios of the years 2000 and 2010 along with auxiliary data (elevation, slope, aspect, distance from sea, and distance from river) were considered. In a simulation model, auxiliary datasets are used to give context, limitations, and insights into the different aspects that affect decisions about land use. These datasets help the

model to become more realistic by enhancing accuracy and effectiveness. The followed simulation process was cell-based and each cell had a particular number of variables depending on the number of input data. These variables can be understood by the following equation:

$$C = [m_1, m_2, m_3 \dots, m_n]^T \dots \dots \dots iv$$

Where, c refers to a particular cell which contains  $m_1$  spatial variables and T stands for transposition. Once the inputs were set, correlation among the variables were calculated using *Pearson’s correlation method* and changes among the land use categories within the selected years (2000 and 2010) were assessed by comparing two land use raster. A transitional matrix was produced to check the exchange pattern among LULC classes and calculate absolute changes within the classes.

The next step was LULC transitional probability modelling using ANN. Where, In the first layer, each



spatial variable was counted as a neuron, which is referred to as an input. By the channels, these neurons will be linked next layer. A weight, which is a number, is assigned to every single channel. The inputs get multiplied by the matching weight, and sum is sent as an input to the hidden layer. The hidden layer mechanism can be shown as follows:

$$\text{net } j(k, t) = (Wx(k, t))[i] \dots\dots\dots v$$

W refers to weight of the channel that connects input neurons with the neuron j in the hidden layer. x(k,t) is the result of the input layer at time t. The notation i is the i-th element of the output which is associated with

the net input neuron j. Through continuous function across the channel, these neurons subsequently transmit the data to the output layer. The neuron with the greatest value in the output layer delivers the desired result. The idea can be expressed as follow:

$$P(y, t, l) = f \left( W_1 \cdot f \left( W_2 \cdot x(y, t) \right) \right) \dots\dots\dots vi$$

Where P(y, t, l) is the probability of the y th cell having the lth variation of LULC at period t. f is the continuous function. W denotes weight, while x(y,t) signifies the input of the y-th cell at period t.

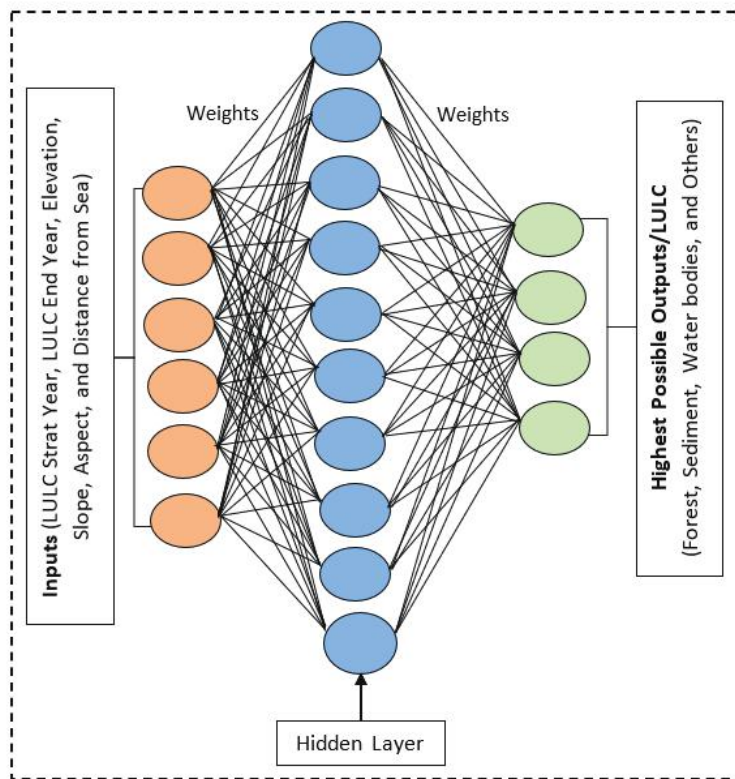


**Figure 2:** The Conceptual Framework of the Artificial Neural Network-based Cellular Automata was Used to Simulate LULC Scenario for the Year 2031, (The Model was Configured with 3 px Neighborhood, 0.10 Learning Rate, 1000 Iterations, 10 Hidden Layers, and 0.050 Momenta to Find Out the Balance Between Model Complexity and Performance While Training and Testing. These Parameters’ Impact on the Behavior and Performance of the Model Makes them Crucial to the Simulation)

The model also used backward propagation to adjust the incorrect prediction. This backward propagation functions till the system accurately predicts most of the outcomes. However, following the transitional probability, CA simulation was conducted for the year 2021. The result was then validated comparing the output with the reference LULC map of 2021. The

validation steps were assessed using Kappa coefficient and overall accuracy assessment techniques. The validated model was used to predict the result for the year 2031. To apply this model, the MOLUSCE plug-in of QGIS 2.18.0 was utilized. Figure 2 represents the conceptual framework of the simulation model used.



**Table 2:** Different Accuracy Indicators Representing the Accuracy Level of the Classified Images for the Years 2000 to 2021 (UA= User; PA= Producer; OA= Overall; K= Coefficient)

Time	LULC Classes	UA (%)	PA (%)	OA (%)	K
2000	Forest	86.36	88.79	89.76	0.86
	Sediment	90	94.74		
	Water Bodies	91	91.09		
	Others	92	85.05		
2007	Forest	84	89.36	85.5	0.81
	Sediment	88	80.73		
	Water Bodies	83	86.46		
	Others	87	86.14		
2010	Forest	82.08	85.29	83.25	0.78
	Sediment	86	80.37		
	Water Bodies	83	83.84		
	Others	82	83.67		
2016	Forest	91	91.92	91.75	0.89
	Sediment	93	91.18		
	Water Bodies	89	93.69		
	Others	94	90.39		
2021	Forest	95.92	90.07	92.21	0.90
	Sediment	88	93.62		
	Water Bodies	90	92.78		
	Others	95	89.62		

### ANN Model Validation

To achieve a good simulation or prediction result, it is important to follow the training and validation steps. The classified images of 2000, 2010, and 2021 were used for training and validation of the selected model. Since this model does not take input with different specifications, all selected data (both main inputs and auxiliary inputs or variables) were processed maintaining the same geometric registration (reference system) and extent (pixel size). After preparing data

for the model, the first step was training the model, to do so, together with the classified land use of the years 2000 and 2010; auxiliary data (elevation, slope, and aspect) were used as the model inputs. Based on these inputs, a land cover scenario for the year 2021 was produced. While producing this initial result (2021), all the parameters of ANN were modified as a process of model configuration until the result was satisfactory. For example, the same model was tested with three different neighborhood functions (3x3, 5x5, 7x7), and each function showed a different output.

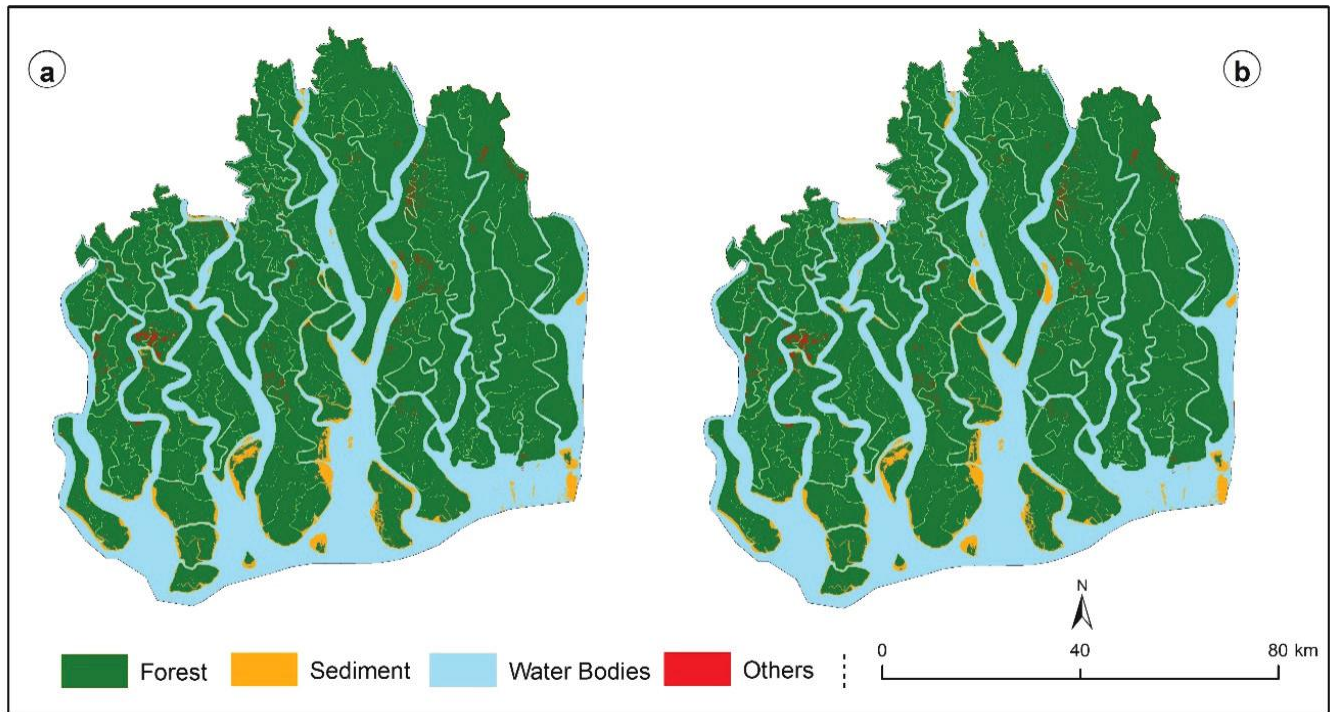


**Figure 3:** Comparison of the Model's Validation Outputs with Referenced Land Cover Map: a) Reference/Original Land Use Map 2021, b) Simulated Land Use Map 2021

Since a land cover scenario for the year 2021 was prepared before, there was an opportunity to compare it with the simulated result to validate the model; thus, considering 2021 as the reference year, the model was validated. The accuracy level of the 3x3 function at the validation stage was higher than the other two functions. The 3x3 function simulated a result with 95.76% accuracy, where 5x5 and 7x7 were able to produce with 89.52 % and 87.83% accordingly. So, with the 3x3 function, the model was considered the best fit, where the learning rate and momentum were 0.10 and 0.050, respectively. An evaluation of the reference and simulated land cover maps of 2021 showed there was no noticeable difference between these two land cover maps (Fig. 3). According to Table 3, the quantity of different land covers showed less variation, although the difference in forest covers was about 2 km<sup>2</sup>. More precisely, forest cover in the simulated year was 3967.27 km<sup>2</sup>, and in the reference year, it was 3969.33 km<sup>2</sup>.

**Table 3:** Quantitative Difference between Referenced Land Cover and Simulated Land Cover of Sundarbans in 2021 (This Result was Produced Based on the Model's Validation Outputs Using ArcMap)

Types	Referenced land cover 2021 (sq.km)	Simulated land cover 2021 (sq.km)	Difference (sq.km)
Forest	3969.33	3967.27	-2.06
Others	24.53	25.08	0.55
Sediment	128.46	130.12	1.66
Water Bodies	1780.10	1779.94	-0.16
Total	5902.42	5902.42	0

### LULC Scenario of Sundarbans (2000 to 2021)

Table 4 and Figure 3 show the land cover in the study area from 2000 to 2021. In all these years forest was the most dominating land cover with an area coverage of around 4000 sq. km. In the initial year (2000), the forest cover was 4036.92 sq. km, which reached 3969.33 sq. km in the final year (2021). After 2000, forest cover increased to 4056.08 sq. km in 2007, but by the year 2010, it started to lose its area coverage, and in 2016 the figure reached 3914.79 sq. km, which was about 66.33% of the total land cover.

The second major land cover was water bodies; it covered around 30% of the total area within the study period. Like the forest, the area coverage of water



bodies also fluctuated. In 2000, there was 1801.75 sq. km of water bodies, whereas this figure was 1680.95 sq. km in 2007. Within the selected timeframe, the water

bodies reach their peak in 2016; the quantity of land under water bodies was 1816.64 sq. km responsible for 30.78 % of the total area.

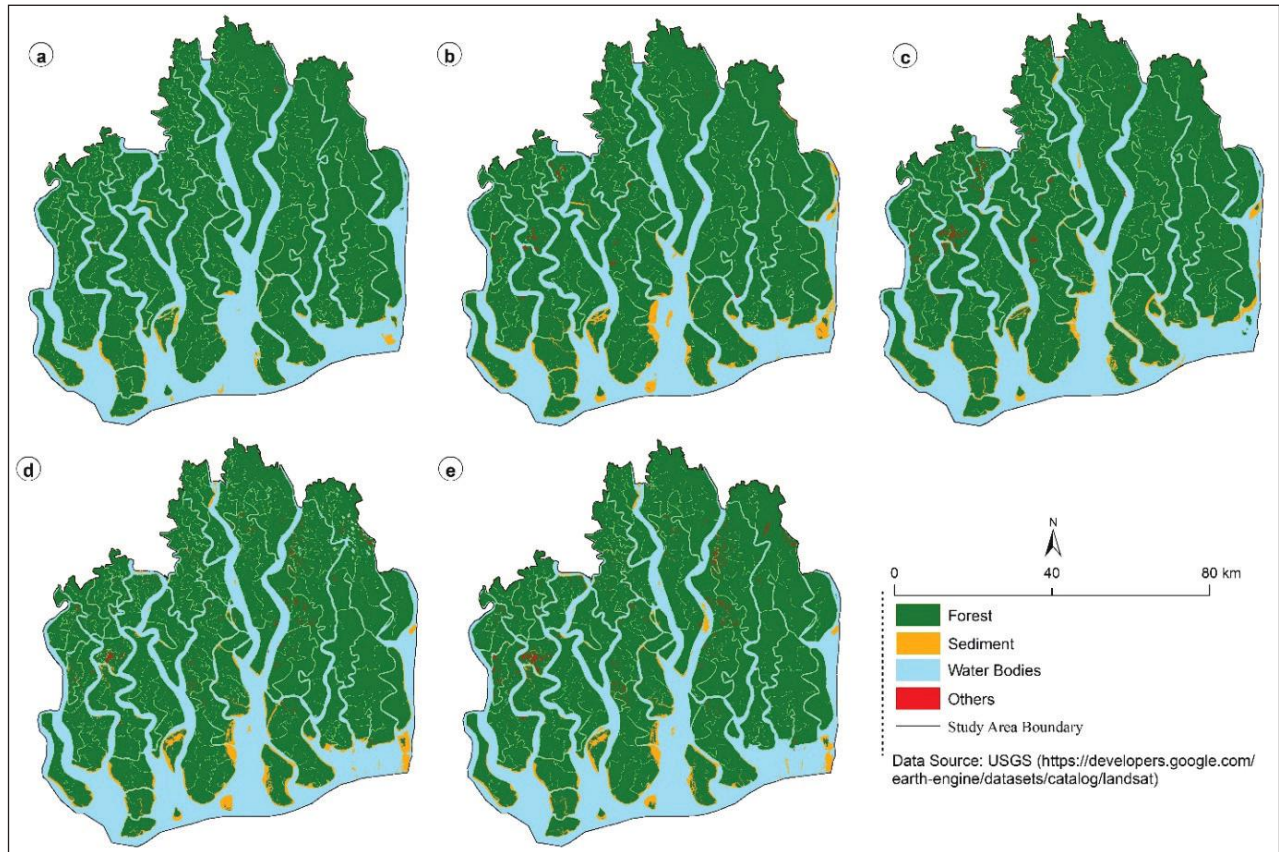


**Figure 4:** Land Covers Map of Sundarbans from 2000 to 2021: (a) 2000, (b) 2007, (c) 2010, (d) 2016, and (e) 2021

Sediment also followed the same trend as forest and water bodies, as its area cover also fluctuated throughout the timeframe. With 61.83 sq. km area coverage in

2000, it placed its mark at 128.46 sq. km in 2021. In the middle; it was 157.56, 121.54, and 153.03 sq. km in 2007, 2010, and 2016, accordingly.

**Table 4:** Land Use Land Cover Changes of the Sundarbans from 2000 to 2021

LULC Types	2000		2007		2010		2016		2021	
	Area (km <sup>2</sup> )	%	Area (km <sup>2</sup> )	%	Area (km <sup>2</sup> )	%	Area (km <sup>2</sup> )	%	Area (km <sup>2</sup> )	%
Forest	4036.92	68.39	4056.08	68.72	4014.81	68.02	3914.79	66.33	3969.33	67.25
Sediment	61.83	1.05	157.56	2.67	121.54	2.06	153.03	2.59	128.46	2.18
Water Bodies	1801.75	30.53	1680.95	28.48	1749.72	29.64	1816.64	30.78	1780.1	30.16
Others	1.91	0.03	7.83	0.13	16.35	0.28	17.95	0.3	24.53	0.42
<b>Total</b>	5902.42	100	5902.42	100	5902.42	100	5902.42	100	5902.42	100

To see the changes more clearly, the year 2000 was considered as the base year. Considering this base year, the study period was divided into four stages: a) 2000 to 2007, b) 2007 to 2010, c) 2010 to 2016, and d) 2016

to 2021. Between 2010 and 2016, the biggest change in mangrove forests took place (Table 5). During this time Sundarbans lost more than 100 sq. km of the forest. Besides, 41.27 sq. km of forest land was also

lost from 2007 to 2010. In the first (2000-2007) and last stage (2016-2021), land cover changed into forested

land occurred about 19.16 sq. km and 54.54sq. km respectively.

**Table 5:** Assessment of Changes in different Land Cover (A positive Value Represents the Increment in Areal Extent while a Negative Value Represents the Decrement)

Types	Area	Time
Forest	19.16	2000-2007
Sediment	95.72	
Water Bodies	-120.81	
Others	5.92	
Forest	-41.27	2007-2010
Sediment	-36.02	
Water Bodies	68.77	
Others	8.52	
Forest	-100.02	2010-2016
Sediment	31.49	
Water Bodies	66.92	
Others	1.61	
Forest	54.54	2016-2021
Sediment	-25.58	
Water Bodies	-36.54	
Others	7.58	

Sediment gained most of its land cover between 2000 and 2007, which was 95.72 sq. km. In the next stage (2007 to 2010), it lost about 36.02 sq. km of land cover. From 2010 to 2016, sediment deposition increased by 31.49 sq. km and in the final stage, again the Sundarbans lost about 25.58 sq. km of deposited land. After forested land, some of the biggest changes were also recorded for water bodies. In the beginning, the study area lost about 121 sq. km of water bodies. After losing such a vast quantity of water bodies, there were 68.77 and 66.92 sq. km of recovery in the second and third stages. In the final stage (2016 to 2021), again about 36.54 sq. km loss was recorded. On the other hand, others land over showed a positive trend in all four stages.

**Simulated Land Cover**

**Table 6:** Quantified Simulated Land Cover for the Year 2031

Types	Area	%
Water Bodies	1804.58	30.57
Forest	3913.03	66.30
Sediment	154.73	2.62
Others	30.08	0.51
<b>Total</b>	<b>5902.42</b>	<b>100</b>

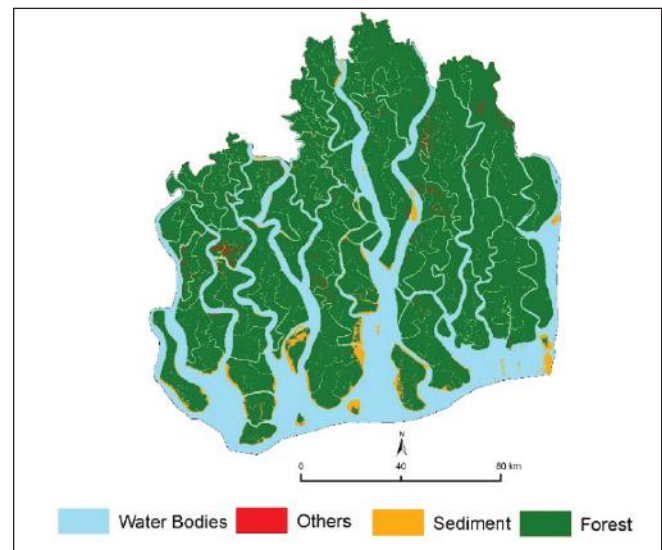


**Figure 5:** Simulated Land Cover Scenario for the Year 2031

The simulated result shows that, by the year 2031, there will be 3913.03 sq. km of forest covering an area of about 66.30% of the total area.

Figure 5 and Table 6 are also showing that water bodies will remain the second most dominating land cover

in the study area 1804.58 sq. km of land coverage. Besides, there will be 154.73 sq. km of sediment and 30.08 sq. km of other land covers.

**Transitional Change of LULC (2000 to 2031)**

To identify the detailed changes both in the past and future land cover, transitional changes among the land cover divided into two different periods were

analyzed; a) 2000 to 2021, and b) 2021 to 2031. This transitional analysis helps to identify changes among the land cover groups that comprise the total change scenario. Looking at the forest cover, most of the forest land was turned into water bodies from 2000 to 2021 and the same trend will be taken place from 2021 to 2031. In the first period of transition, the quantity of lost forest land was about 79.79sq.km and in the second period it will be 77.33sq. km.

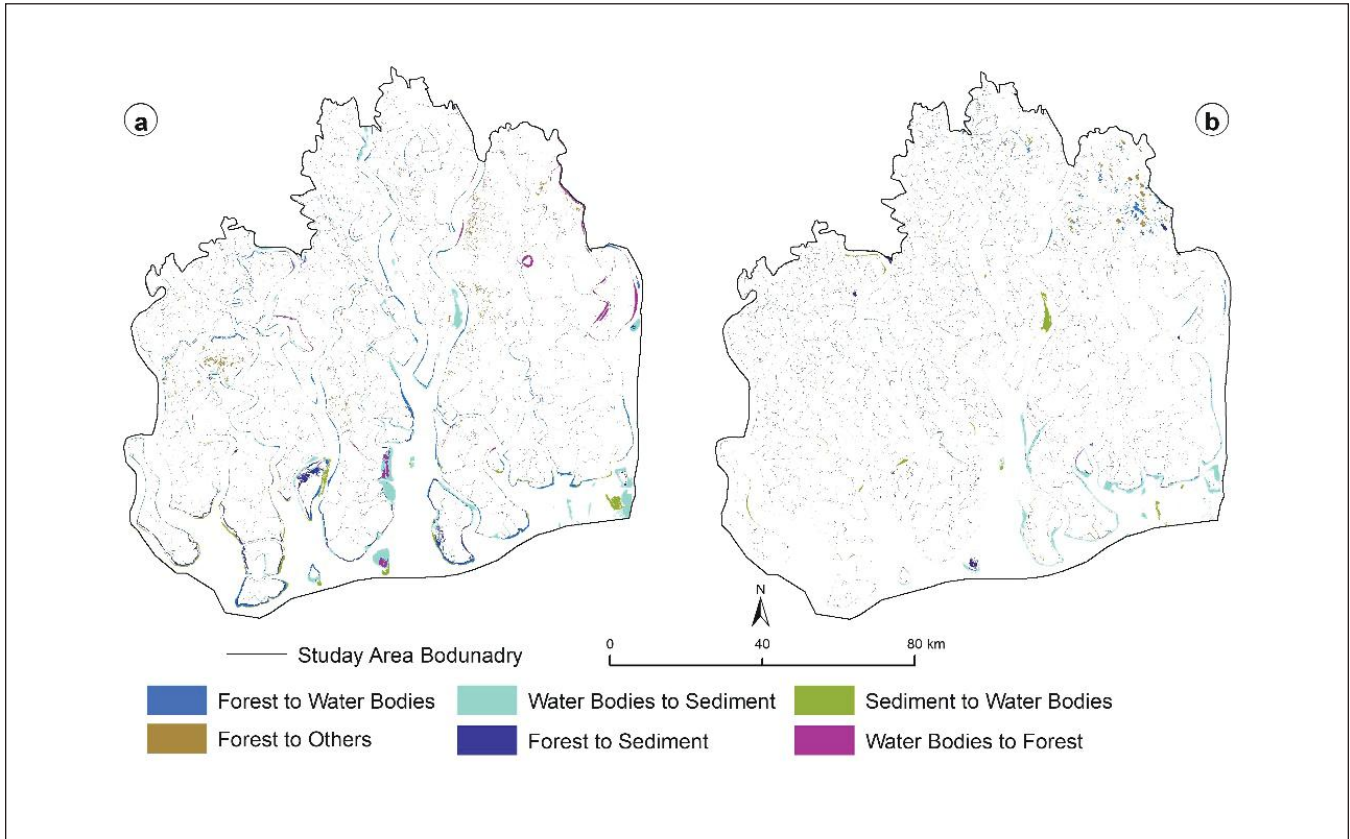


**Figure 6:** Major Transitional Changes among Land Cover Classes from 2000 to 2031: (a) 2000 to 2021, (b) 2021 to 2031

A considerable portion of forested land was changed into sediment and other land covers in both periods. On the contrary, forest land recovered most of its land from water bodies in both of the periods. According to Figure 6 and Table 7, like forest land, sediment also lost and gained most of its land cover in water bodies. Moving on to the water bodies, it lost most of its area to sediments and the quantities of loss were 69.71 and

38.49 sq. km. Besides, water bodies also lost 60.92 sq. km of land cover to a forested area from 2000 to 2021, and from 2021 to 2031 the figure will be 28.69 sq. km. Finally, looking at the other land cover, there was no remarkable change from 2000 to 2021. From 2021 to 2031, 7.74 sq. km of other land covers will be turned into forested land and most of the land will be recovered from forest.

**Table 7:** Quantitative Transitional Change within the Land Covers Classes from 2000 to 2031

Transition Types	Area (2000 to 2021)	Area (2021 to 2031)
Unchanged Forest	3900.33	3871.58
Forest to Others	22.26	13.30
Forest to Sediment	34.54	8.85
Forest to Water Bodies	79.79	77.33
Others to Forest	0.67	7.74
Unchanged Others	0.91	15.07
Others to Sediment	0.24	1.04
Others to Water Bodies	0.08	0.69
Sediment to Forest	7.41	4.87
Sediment to Others	0.01	0.67
Unchanged Sediment	23.96	106.29
Sediment to Water Bodies	30.45	16.60
Water Bodies to Forest	60.92	28.69
Water Bodies to Others	1.34	0.45
Water Bodies to Sediment	69.71	38.49
Unchanged Water Bodies	1669.78	1710.77

### Factors of LULC Changes in the Sundarbans According to Local People

Summary statistics were calculated in R studio to identify respondents' profiles. Most of the respondents were male (Table 8). In terms of age, more than 50% of the respondents were in the age group of 30 to 50 years and over 50 years was the second-largest age bracket. Five categories of respondents were found from the perspective of education level. About 14% of the surveyed respondents did not receive any formal education and only 4 respondents had managed to get the graduation. The education level of the majority

ranges from primary (37.50%) to secondary (32.50%). Respondents were from eight different professions. Farming was the primary occupation which comprised 50% of the overall responses. Fifteen respondents were engaged in agribusiness. This study wanted to extract the root causes of changes in the Sundarbans by maintaining professional diversity. Therefore, in addition to the farmer and agribusiness man, the survey data was also collected from housewives, businessmen, fishermen, labourers, government employees, and private service holders, where the number of housewives (12 out of 80) was higher than the other five professionals.



**Table 8:** Demographic Profile of the Surveyed Respondents (A Total of Five Variables were Identified to Summarise the Demographic Profile of the Respondents)

Variable	Category	Observation (n=80)	Percentage
Gender	Male	55	68.75
	Female	25	31.25
Age	<30	11	13.75
	30-50	50	62.50
	>50	19	23.75
Education	Uneducated	11	13.75
	Primary	30	37.50
	Secondary	26	32.50
	Higher Secondary	13	16.25
	Graduate	4	5.00
Profession	Farmer	20	25.00
	Agribusiness	15	18.75
	Housewife	12	15.00
	Business	9	11.25
	Fisherman	8	10.00
	Labor	8	10.00
	Government Employee	5	6.25
	Private Service	3	3.75

80 local respondents were interviewed to identify the root causes of the land cover changes in Sundarbans where a total of 13 driving factors of changes were identified in this survey (Fig. 7). According to the majority, the cyclones are considered the prominent cause of the LULC change in Sundarbans. About 16.25 percent of local people agreed that every year the Sundarbans is badly affected by cyclone. As a result, the cyclone left its mark on the Sundarbans mangrove ecosystem, hazardous repercussions on vegetation and inflicting major erosion along the shoreline (Mishra et al., 2021). Also, for the last two decades, the number of natural hazards has increased at a drastic rate (Kundu et al., 2021). About 13 percent of respondents claimed that deforestation is another big reason for the changes in Sundarbans. In various studies, it has been found that the deforestation rate is higher than the reforestation rate in South Asia (Kundu et al., 2021). According to the local people, the other causes of the spatio-temporal changes in Sundarbans could be pollution, coastal erosion, overexploitation, climate change, shrimp farming, development activities, diseases, and sediment deposition by 11.25%, 10.00%, 8.75%, 7.50%, 7.50%, 6.25%, 5.00% and 5.00% accordingly of the total 80 respondents (Table 9). Very few respondents (less than 5%) of the study area marked some causes as

driving factors of the changes in Sundarbans. Those were industrial activity, fire and tourism by 3.75%, 2.50%, and 2.50% respondents respectively.



**Figure 7:** Word Cloud Representing the Causes of Land Cover Changes in the Sundarbans According to the Respondents

**Table 9:** Percentage of the Respondents' Opinions on different Causes of Change in the Land Cover of the Sundarbans

Variables	Percentage
Cyclone	16.25
Deforestation	13.75
Pollution	11.25
Coastal erosion	10.00
Overexploitation	8.75
Climate change	7.50
Shrimp farming	7.50
Development activities	6.25
Diseases	5.00
Sediment deposition	5.00
Industrial activity	3.75
Fire	2.50
Tourism	2.50
Total	100

The respondents were asked to mark the influence level of these reasons or factors they mentioned following a Likert scale. In survey research, particularly in social science research, the Likert scale is the most often used scale (Pimentel, 2010). However, there were five possibilities on the scale to choose from: very low influence, moderate influence, medium influence,

strong influence, and very high influence. At least one hypothesis springs in mind to test with this Likert scale's outputs. To do so, a sampled T-test with a 95% confidence interval was done because  $H_0$  was all these factors influencing the Sundarbans significantly. i.e., the mean of  $x$  is greater than 3 (medium influence).

**Table 10:** Summary of Multiple Linear Regression Model

Indicators	Estimate	Std Error	Value (t)	Pr(> t )
(Intercept)	5.5885	0.74604	7.491	1.18E-10*
Gender	-0.25542	0.24837	-1.028	0.307
Ethnicity	-0.18904	0.21978	-0.86	0.392
Age	-0.01427	0.00921	-1.55	0.125
Education	-0.1154	0.11781	-0.98	0.33
Occupation	-0.06032	0.04862	-1.241	0.219
Number of Observations R <sup>2</sup>	800.01569			

The result revealed that the  $\bar{x}$  is 3.875, which means that the factors mentioned by the participants are highly responsible for land cover changes in this largest mangrove forest.

By hypothesis testing, the relationship between heterogeneity in respondents' opinions on influence level and factors associated with the respondents was checked using a multiple linear regression model (equation viii). The result showed that there was no connection between respondents' opinions and factors

associated with them (Table 10). So, heterogeneity might be caused by other factors like distance from the study area.

## DISCUSSION

In recent years land use and land cover change in Sundarbans have occurred significantly. However, it has been estimated that losing rate of forest land is higher than other LULC types, while this study shows

from 2000 to 2021; only 1.14% of the total forest land was lost (Table 4). Many studies reported that this loss rate has been decreasing from the previous decades, and from 1990 to 2000, it was around 1.2% (Giri et al., 2007; Dasgupta et al., 2019; Sardar and Samaddar, 2021). The findings also show that the forest area will decrease in 2031 although it would be the most dominating land cover (Table 7) of the study area as it is now.

Coastal Bangladesh suffered from some major cyclones in the last two decades (Mahmood et al., 2021), which resulted in some erosion and accretion in the Sundarbans. The study shows that in 2021 (Table 4), the sedimentation cover was around 2.18% of the total study area. It was recorded that one of the islands in the southern Sundarbans disappeared in 2010 (Fig. 4c), while in 2016 it reappeared (Fig. 4d). Most of the sediments were deposited in the southern part of the study area, where water meets the land and forest and the main reason for its fluctuation is the fragility to water tide. Other land covers were also stretched within a considerable portion, although the percentage of area coverage was less than 1% in all of the years. The remarkable aspect of other land covers is that it increased steadily; hence, it took a different trend than forest, sediment, and water bodies.

The biggest change in mangrove forests took place between 2010 and 2016. During this period the highest quantity of forest land was lost (Table 5) as cyclone Aila (2009) affected the Sundarbans severely; while in the next period (from 2016 to 2021), a considerable portion of sediment was lost as two major cyclones (Bulbul, 2019 and Amphan, 2020) affected the Sundarbans (Mahmood et al., 2021).

Now, to detect LULC changes, geospatial technologies play a crucial role, but sometimes it is difficult to identify through these technologies whether these changes are caused by humans or nature. Considering this fact, this study has incorporated the local people's perception of the changes in the Sundarbans.

Locals believe that the land use and land cover changes in Sundarbans are mainly caused by the cyclone (Table 9, Fig. 7). Deforestation and over-exploitation (according to about 13% and 8 % of respondents respectively) are also among the major causes of LULC changes in this area (Table 9). About 7.5% of the total respondents agreed that shrimp farming has a huge impact on the changing land use practice of the study area.

Due to the development of transport facilities in recent years, the mangrove has been a favourite destination place for many national and international tourists (Uddin, 2011; Kumar, 2015; Mahmood et al., 2021). The local residents (around 2.5%) also marked this as a reason for land use changes in the study area.

## CONCLUSIONS

It can be concluded that the Sundarbans is suffering from various natural and manmade disturbances that will continue in the future if a proper management plan is not considered. The findings of the present study demonstrate that the land covers in this study are quite dynamic, a fluctuating trend in changes from year to year can be observed and this trend will be continued. Moreover, this study reiterates that cyclones, deforestation, pollution, coastal erosion, over-exploitation of resources, climate change, shrimp farming, development activities, and diseases are some of the main driving factors that control changes in the mangrove forests. Therefore, these findings could be used as a baseline for nature conservation and will provide valuable information for stakeholders, decision-makers, and policy experts.

## REFERENCES

- Abdullah, A. Y. M., Masrur, A., Adnan, M. S. G., Baky, M. A. A., Hassan, Q. K., Dewan, A., 2019. Spatio-temporal patterns of land use/land cover change in the heterogeneous coastal region of Bangladesh between 1990 and 2017. *Remote Sensing* 11(7), 790. doi.org/10.3390/rs11070790
- Akbar Hossain, K., Masiero, M., Pirotti, F., 2022. Land cover change across 45 years in the world's largest mangrove forest (Sundarbans): the contribution of remote sensing in forest monitoring. *European Journal of Remote Sensing* 1-17. doi.org/10.1080/2797254.2022.2097450
- Baig, M., Mustafa, M., Baig, I., Takaijudin, H., Zeshan, M., 2022. Assessment of land use land cover changes and future predictions using CA-ANN simulation for Selangor, Malaysia. *Water* 14(3), 402. doi.org/10.3390/w14030402
- Biswas, P. L., Biswas, S. R., 2019. Mangrove forests: ecology, management, and threats. *Life on Land* 1-14. doi.org/10.1007/978-3-319-71065-5\_26-1

- Carugati, L., Gatto, B., Rastelli, E., Lo Martire, M., Coral, C., Greco, S., Danovaro, R., 2018. Impact of mangrove forests degradation on biodiversity and ecosystem functioning. *Scientific Reports* 8(1). doi.org/10.1038/s41598-018-31683-0
- Chowdhury, M., Hafsa, B., 2022. Multi-decadal land cover change analysis over Sundarbans Mangrove Forest of Bangladesh: A GIS and remote sensing-based approach. *Global Ecology and Conservation* 37. doi.org/10.1016/j.gecco.2022.e02151
- Dasgupta, S., Islam, M.S., Huq, M., Khan, Z.H., Hasib, M.R., 2019. Quantifying the protective capacity of mangroves from storm surges in coastal Bangladesh. *PloS One* 14 (3): e0214079. doi.org/10.1371/journal.pone.0214079.
- Debanshi, S., Pal, S., 2020. Wetland delineation simulation and prediction in deltaic landscape. *Ecological Indicators* 108, 105757. doi.org/10.1016/j.ecolind.2019.105757
- FAO (Food and Agriculture Organization of the United Nations), 2007. The world's mangroves 1980–2005. FAO Forestry Paper. Forestry Economics and Policy Division, FAO, Rome. <http://www.fao.org/documents/card/en/c/880053ed-9752-5939-b242-35fd7603a2ba/> (accessed 20.09.2022).
- Faruque, M.J., Vekerdy, Z., Hasan, M.Y., Islam, K.Z., Young, B., Ahmed, M.T., Monir, M.U., Shovon, S.M., Kakon, J.F., Kundu, P., 2022. Monitoring of land use and land cover changes by using remote sensing and GIS techniques at human-induced mangrove forests areas in Bangladesh. *Remote Sensing Applications: Society and Environment* 25, 100699. doi.org/10.1016/j.rsase.2022.100699
- Ghosh, A., Schmidt, S., Fickert, T., Nusser, M., 2015. The Indian Sundarban mangrove forests: History, utilization, conservation strategies, and local perception. *Diversity* 7 (2), 149–169. doi.org/10.3390/d7020149
- Giri, C., Ochieng, E., Tieszen, L. L., Zhu, Z., Singh, A., Loveland, T., Masek, J., Duke, N., 2010. Status and distribution of mangrove forests of the world using earth observation satellite data. *Global Ecology and Biogeography* 20(1), 154–159. doi.org/10.1111/j.1466-8238.2010.00584.x
- Giri, C., Pengra, B., Zhu, Z., Singh, A., Tieszen, L., 2007. Monitoring mangrove forest dynamics of the Sundarbans in Bangladesh and India using multi-temporal satellite data from 1973 to 2000. *Estuarine, Coastal and Shelf Science* 73(1-2), 91–100. doi.org/10.1016/j.ecss.2006.12.019
- Gopal, B., Chauhan, M., 2006. Biodiversity and its conservation in the Sundarban Mangrove Ecosystem. *Aquatic Sciences* 68(3), 338–354. doi.org/10.1007/s00027-006-0868-8
- Hasan, M., Nath, B., Sarker, A., Wang, Z., Zhang, L., Yang, X., Nobi, M., Røskoft, E., Chivers, D., Suza, M., 2020. Applying multi-temporal landsat satellite data and Markov-cellular automata to predict forest cover change and forest degradation of Sundarban Reserve Forest, Bangladesh. *Forests* 11(9), 1016. doi.org/10.3390/f11091016
- Halmy, M. W. A., Gessler, P. E., Hicke, J. A., Salem, B. B., 2015. Land use/land cover change detection and prediction in the North-western coastal desert of Egypt using Markov-CA. *Applied Geography* 63, 101–112. doi.org/10.1016/j.apgeog.2015.06.015
- Islam, M. M., Borgqvist, H., Kumar, L., 2019. Monitoring mangrove forest landcover changes in the coastline of Bangladesh from 1976 to 2015. *Geocarto International* 34(13), 1458–1476. doi.org/10.1080/10106049.2018.1489423
- Kumar, F., 2015. Assessment of tourist carrying capacity of different tourist spots (Kotka, Kochikhali, Hironpoint, Dubla, Harbaria, Koromjol and Kolagachia) of the Sundarbans. MS Thesis. Forestry and Wood Technology Discipline, Khulna University, Khulna, Bangladesh.
- Kundu, K., Halder, P., Mandal, J.K., 2021. Change detection and patch analysis of Sundarban forest during 1975–2018 Using Remote Sensing and GIS data. *SN Computer Science* 2(5), 1-14. doi.org/10.1007/s42979-021-00749-8
- Li, X., Yeh, A.G.O., 2002. Neural-network-based cellular automata for simulating multiple land use changes using GIS. *International Journal of Geographical Information Science* 16(4), 323-343. doi.org/10.1080/13658810210137004
- Mahmood, H., Ahmed, M., Islam, T., Uddin, M. Z., Ahmed, Z. U., Saha, C., 2021. Paradigm shift in the management of the Sundarbans mangrove forest of Bangladesh: Issues and Challenges. *Trees, Forests and People* 5, 100094. doi.org/10.1016/j.tfp.2021.100094



- Mehta, A., Sinha, V., Ayachit, G., 2012. Land-use/land-cover study using Remote Sensing and GIS in an Arid Environment. *Bulletin of Environmental and Scientific Research* 1(3-4), 4-8. <http://besr.org.in/index.php/besr/article/view/29> (accessed 09.10.2022).
- Mishra, M., Acharyya, T., Santos, C., Silva, R., Kar, D., Mustafa Kamal, A., Raulo, S., 2021. Geocological impact assessment of severe cyclonic storm Amphan on Sundarban mangrove forest using geospatial technology. *Estuarine, Coastal and Shelf Science*. doi.org/10.1016/j.ecss.2021.107486
- Mountrakis, G., Im, J., Ogole, C., 2011. Support vector machines in remote sensing: A review. *ISPRS Journal of Photogrammetry and Remote Sensing* 66(3), 247–259. doi.org/10.1016/j.isprsjprs.2010.11.001
- Orimoloye, I. R., Kalumba, A. M., Mazinyo, S. P., Nel, W., 2020 Geospatial analysis of wetland dynamics: Wetland depletion and biodiversity conservation of Isimangaliso Wetland, South Africa. *Journal of King Saud University – Science* 32(1), 90-96. doi.org/10.1016/j.jksus.2018.03.004
- Parsa, V. A., Yavari, A., Nejadi, A., 2016. Spatio-temporal analysis of land use/land cover pattern changes in Arasbaran Biosphere Reserve: Iran. *Modeling Earth Systems and Environment* 2(4), 1–13. doi.org/10.1007/s40808-016-0227-2
- Pimentel, J. L., 2010. A note on the usage of Likert Scaling for research data analysis. *USM R&D Journal* 18, 109-112.
- Polidoro, B.A., Carpenter, K.E., Collins, L., Duke, N.C., Ellison, A.M., Ellison, J.C., Farnsworth, E.J., Fernando, E.S., Kathiresan, K., Koedam, N.E., Livingstone, S.R., Miyagi, T., Moore, G.E., Nam, V.N., Ong, J.E., Primavera, J.H., Salmo, S.G., Sanciangco, J.C., Sukardjo, S., Wang, Y., Yong, J.W.H., 2010. The loss of species: mangrove extinction risk and geographic areas of global concern. *PLoS ONE* 5(4). doi.org/10.1371/journal.pone.0010095
- Quader, M. A., Agrawal, S., Kervyn, M., 2017. Multi-decadal land cover evolution in the Sundarban, the largest mangrove forest in the world. *Ocean & Coastal Management* 139, 113–124. doi.org/10.1016/j.ocecoaman.2017.02.008
- Rahman, M.M., Khan, N. I. M., Hoque, K. F. A., Ahmed, I., 2015. Carbon stock in the Sundarbans mangrove forest: spatial variations in vegetation types and salinity zones. *Wetlands Ecology and Management* 23, 269–283. doi.org/10.1007/s11273-014-9379-x
- Rawat, J.S. Kumar, M., 2015. Monitoring Land Use/Cover Change Using Remote Sensing and GIS Techniques: A Case Study of Hawalbagh Block, District Almora, Uttarakhand, India. *The Egyptian Journal of Remote Sensing and Space Sciences* 18, 77-84. doi.org/10.1016/j.ejrs.2015.02.002
- R-bloggers, 2021. Multiple linear regression made simple. <https://www.r-bloggers.com/2021/10/multiple-linear-regression-made-simple/> (accessed 16.05.2022).
- Sardar, P., Samadder, S., 2021. Understanding the dynamics of landscape of greater Sundarban area using multi-layer perceptron Markov chain and landscape statistics approach. *Ecological Indicators* 121, 106914. doi.org/10.1016/j.ecolind.2020.106914
- Sarker, S. K., Reeve, R., Thompson, J., Paul, N. K., Matthiopoulos, J., 2016. Are we failing to protect threatened mangroves in the Sundarbans world heritage ecosystem? *Scientific Reports* 6(1). doi.org/10.1038/srep21234
- Sarwar, M.G.M., Woodroffe, C.D., 2013. Rates of shoreline change along the coast of Bangladesh. *Journal of Coastal Conservation* 17, 515–526. doi.org/10.1007/s11852-013-0251-6
- Shamsi, S.F., 2010. Integrating linear programming and analytical hierarchical processing in Raster-GIS to optimize land use pattern at watershed level. *Journal of Applied Sciences and Environmental Management* 14(2). doi.org/10.4314/jasem.v14i2.57868
- Spalding, M., Kainuma, M., Collins, L., 2010. *World atlas of mangroves*. Earthscan, London. <https://www.routledge.com/World-Atlas-of-Mangroves/Spalding-Kainuma-Collins/p/book/9781844076574>
- Uddin, M.S., 2011. Economic valuation of Sundarbans mangrove ecosystem services A case study in Bangladesh. M. Sc. Thesis. UNESCO-IHE Institute for Water Education, Delft, the Netherlands.

- USGS. Landsat Normalized Difference Vegetation Index, 2022. <https://www.usgs.gov/landsat-missions/landsat-normalized-difference-vegetation-index> (accessed 13.12.2022).
- Vanetti, M., 2007. Confusion matrix online calculator. <https://www.marcovanetti.com/pages/cfmatrix/?noc=4> (accessed 15.12.2022).
- Yang, X., Chen, R., Zheng, X. Q., 2015. Simulating land use change by integrating ANN-CA model and landscape pattern indices. *Geomatics, Natural Hazards and Risk* 7(3), 918–932. doi.org/10.1080/19475705.2014.1001797
- Zaldo-Aubanell, Q., Serra, I., Sardanyés, J., Alsedà, L., Maneja, R., 2021. Reviewing the reliability of land use and land cover data in studies relating human health to the environment. *Environmental Research* 194, 110578. doi.org/10.1016/j.envres.2020.110578
- Zeshan, M. T., Mustafa, M. R. U., Baig, M. F., 2021. Monitoring land use changes and their future prospects using GIS and ANN-CA for Perak River Basin, Malaysia. *Water* 13(16), 2286. doi.org/10.3390/w13162286